HP-Cyclodextrin Modified Sulphur Quantum Dots for the Fluorescent Cage Sensing of *p*-NP by Structural Matching and PET: a New Sensing Approach

Yining Chang,[a,b] Ran He,[a,b] Runqiu Wang, [a] Yanli Wei*[a] and Li Wang*[a]

a Institute of Environmental Science, Shanxi University, Taiyuan, 030031, China

b School of Chemistry and Chemical Engineering, Shanxi University, Taiyuan, 030006, China

**Corresponding author: Li WangE-mail addresses: wangli@sxu.edu.cn (Li Wang)*

Supporting Information

TABLE OF CONTENTS

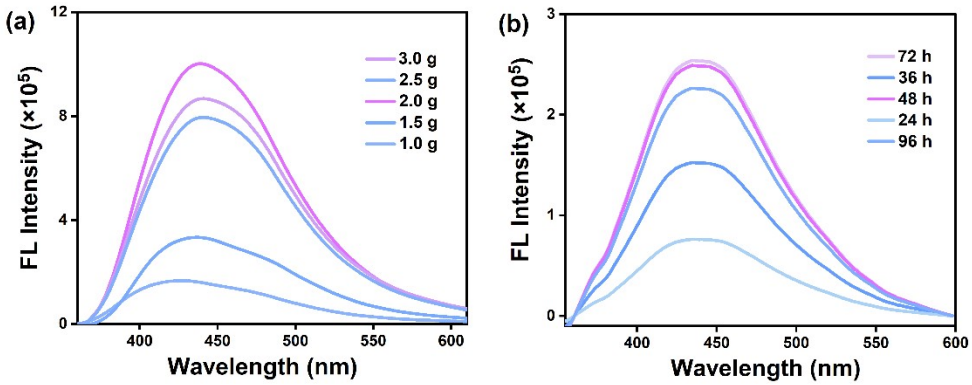

Figure S1 (a)The optimization of the addition amount of HP-β-CD from fluorescent spectrum of SQDs at different concentrations of HP-β-CD. (1.0 g, 1.5 g, 2.0 g, 2.5g, 3.0 g) (b) The optimization of reaction time at 24, 36, 48, 72 and 96 hours.

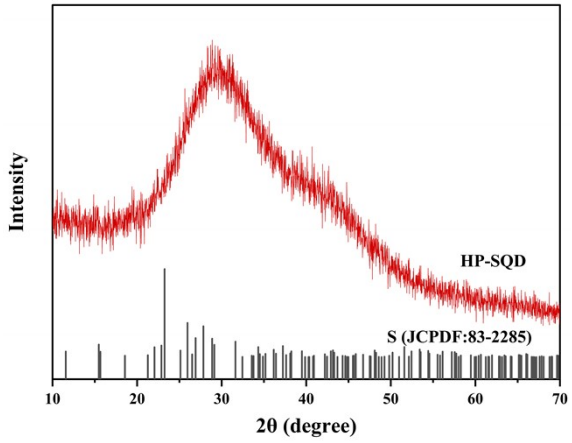

Figure S2 The XRD of HP-SQD.

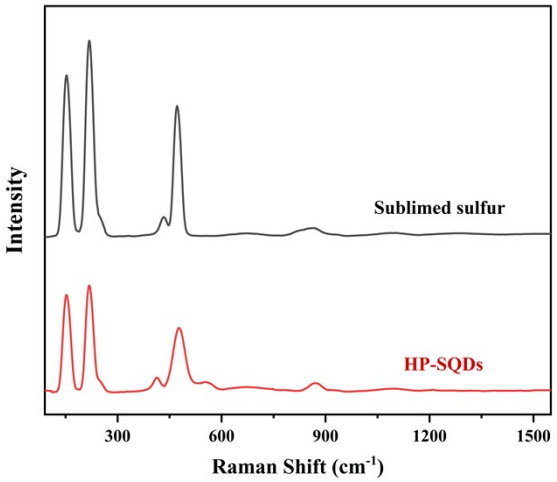

Figure S3 The Raman spectra of HP-SQD.

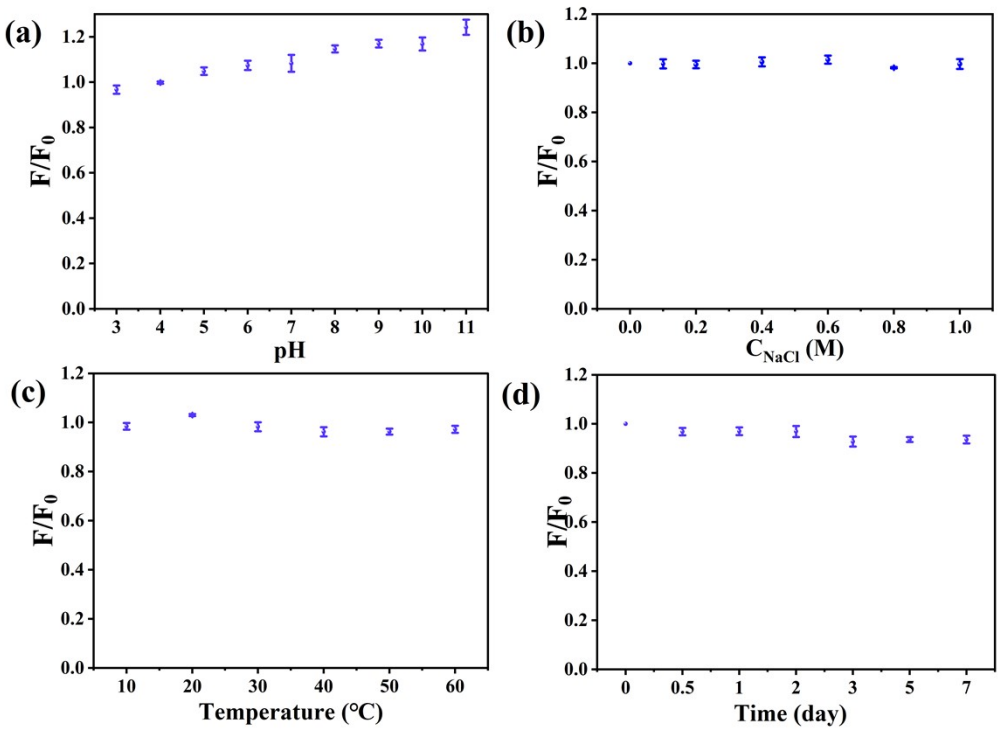

Figure S4 (a) The emission intensity ratio F/F_0 of HP-SQDs at various pH from 3 to11; (b) The effect of NaCl concentration on the intensity ratio F/F_0 in the range from 0.10 to 1.0 M; (c) The effect of temperature change on the intensity ratio F/F_0 from 25 to 60℃; (d) The effect of Storage time at 4°C during seven days after the preparation of HP-SQDs.

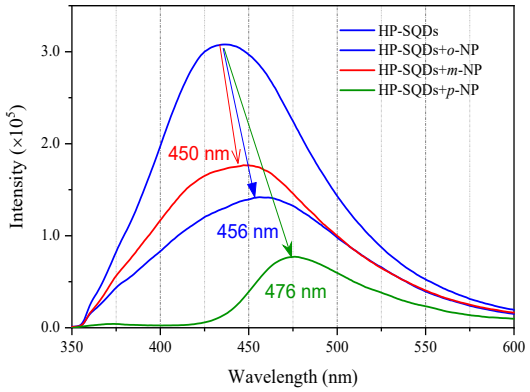

Figure S5 The comparison of emission quenching upon the formation of binding complexes of HP-SQDs with different nitrophenol isomers.

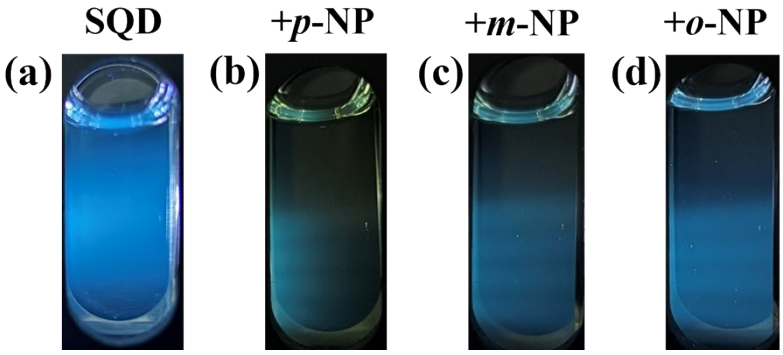

Figure S6 The photo of (a) HP-SQD, (b)SQD + *p*-NP, (c)SQD + *m*-NP, (d) SQD + *o*-NP. (under 365 nm)

Table S1 Compare with other sensors.

Materials	Analytical methods	NPs	Ranges	LODs	Sensing Mechanism	References
Graphene	Electrochemical	*p*-NP	0.5–1250 μM	0.012 μM		[1]
CDs@PDA	Fluorescence	*p*-NP	2.0-34 μM	3.4 μM	IFE	[2]
N-CDs	Fluorescence	*p*-NP	1.0-250 μM	0.40 μM	IFE and Static Quenching	[3]
MIP@CQDs	Fluorescence	*p*-NP	0-114 μM	0.41 μM	IFE and Dynamic Quenching	[4]
perovskite QD	Fluorescence	*p*-NP	0-96 μM	0.16 μM	FRET	[5]
Tb-MOF	Fluorescence	*p*-NP	3.3-46.2 μM	0.415 μM	IFE	[6]
GF/Fe_3O_4	Colorimetric	*p*-NP	0.1-1000 μM	0.045 μM		[7]
MWCNTs	Electrochemical	*p*-NP	1-200 μM	0.41 μM		[8]
Nickel-based	Electrochemical	*p*-NP	0.01-20 nM	7.18 pM		[9]
HP-SQDs	Fluorescence	*p*-NP	2.5-45 μM	0.25 μM	Structural Matching and PET	This Work

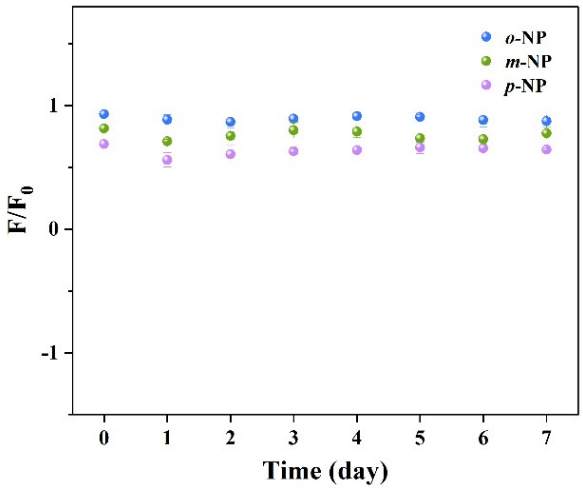

Figure S7 The fluorescence quenching ratio (F/F_0) of the sensor within 7 d.

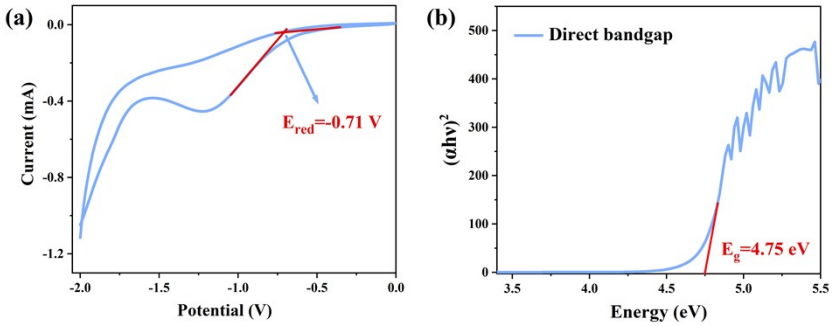

Figure S8 (a) Cyclic voltammogram of the HP-SQDs in 0.1 M $K_2S_2O_8$/PBS solution at 50 mV/s. (b) Optical bandgap of the HP-SQDs obtained from the UV-vis absorption spectrum.

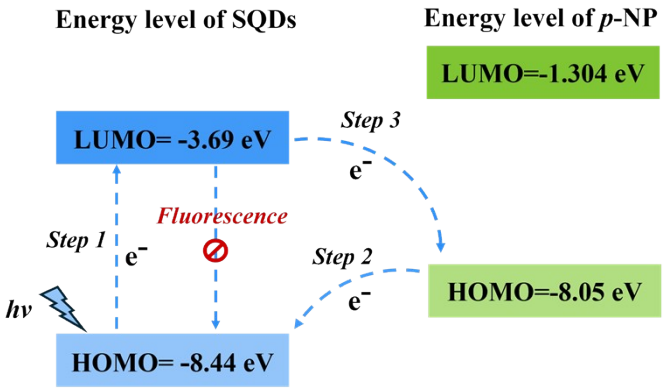

Figure S9 The E_{HOMO} and E_{LUMO} of HP-SQDs and *p*-NP.

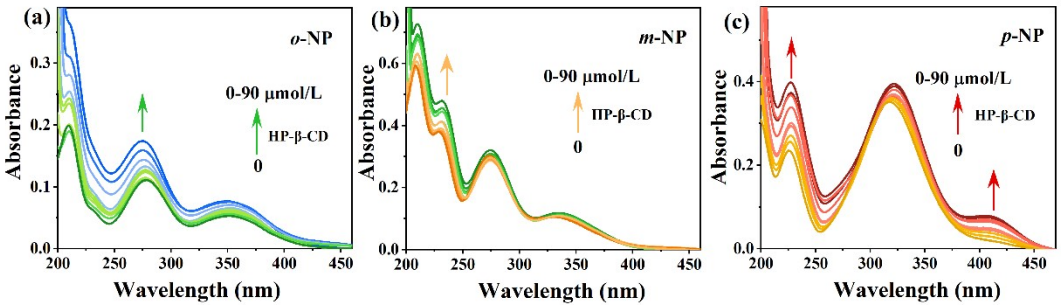

Figure S10 UV-Vis spectral changes (a) *o*-NP, (b) *m*-NP, and (c) *p*-NP at different concentration (0-90 μmol/L) of HP-β-CD. The concentration of nitrophenol is fixed at 40 μmol/L.

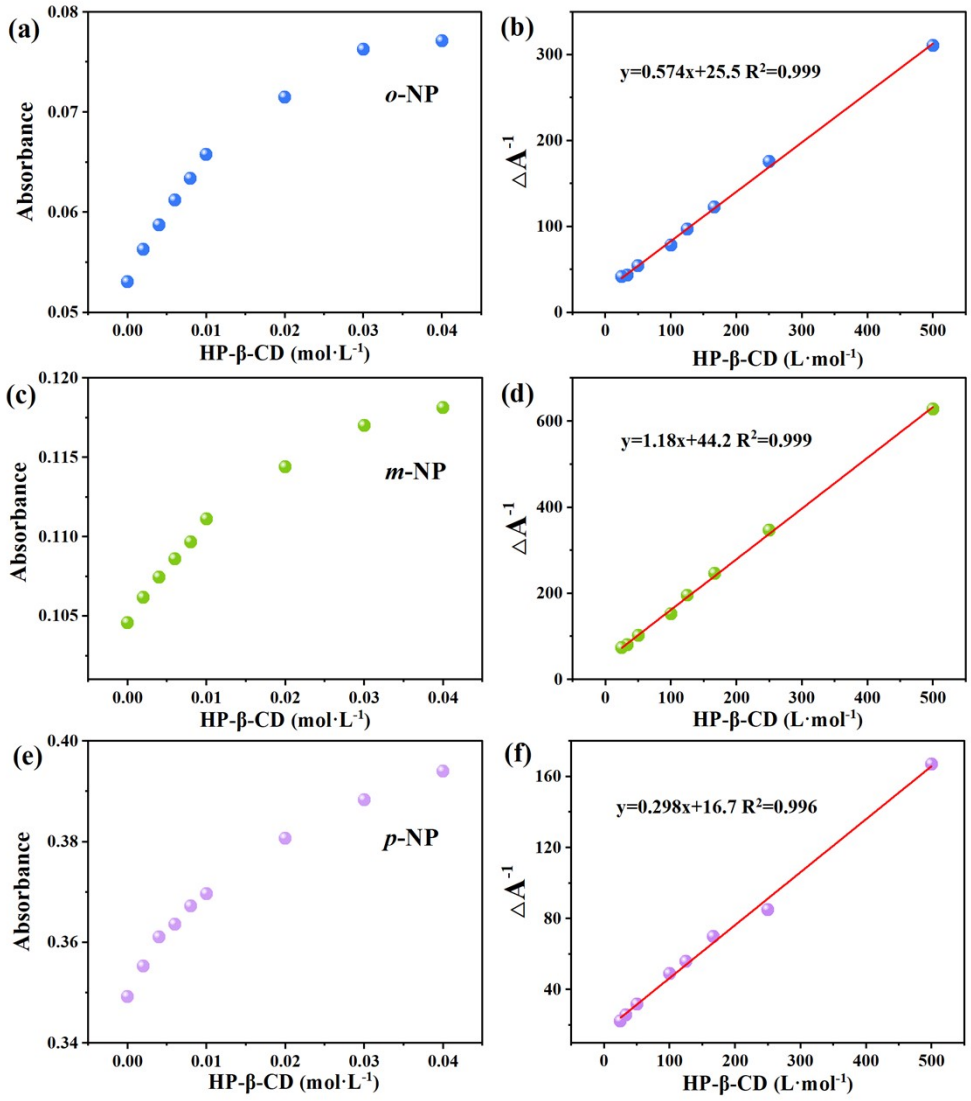

Figure S11 Absorbance changes of (a) *o*-NP, (c) *m*-NP, and (e) *p*-NP with the addition of various concentration of HP-β-CD. The double-reciprocal plot of ΔA^{-1} versus and $[\text{HP-β-CD}]^{-1}$ for *o*-NP/ HP-β-CD (b), *m*-NP/HP-β-CD (d), and *p*-NP/HP-β-CD (f) system.

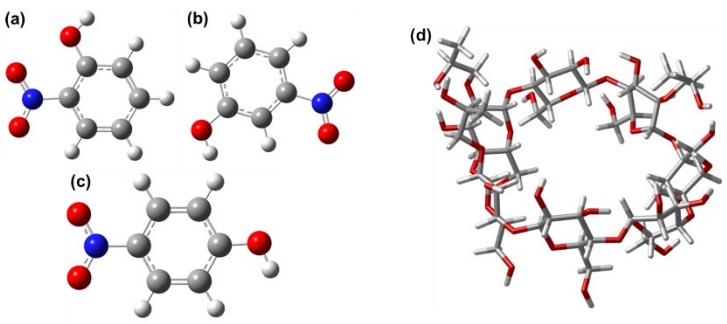

Figure S12 Geometrical structures of (a) *o*-NP, (b) *m*-NP, (c) *p*-NP and (d)2-hydroxylpropyl-β-cyclodextrin molecules optimized at the M062X/6-31G(d) level of theory.

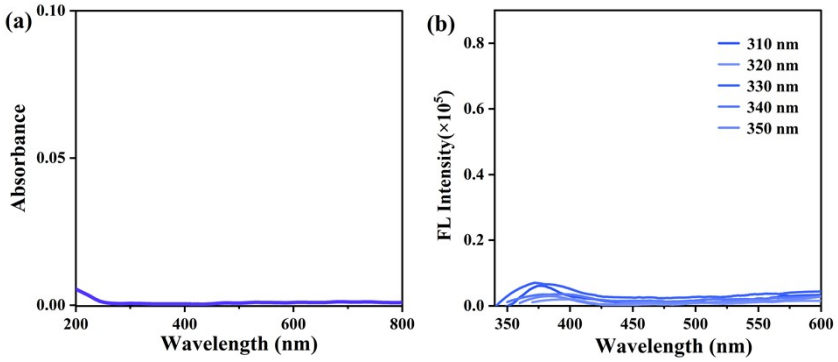

Figure S13 The (a) UV-Vis and (b) fluorescent spectra of mixture(same reaction conditions, no sulphur source added).

Table S2 Complexation energies and free enthalpies of inclusion complexes. All values are in kcal/mol.

	o-NP	*m*-NP	*p*-NP
ΔE	-21.54	-22.15	-24.94
ΔE-BSSE corrected	-11.92	-12.44	-14.63
ΔG	-5.64	-5.53	-6.45

Table S3 Recoveries of nitrophenol isomers for the industrial wastewater (as compared with GC-MS).

Detection	Samples	Spiked (μmol/L)	Found (μmol/L)	Recovery (%)	RSD (%) (n=6)	GC-MS (μmol/L)
	Industrial	0	0	-	-	0
o-NP	Wastewate	40	39.20	98.10	2.04	40.63
	r	60	59.03	98.38	1.04	60.38

		80	78.62	98.28	1.36	80.26
m-NP	Industrial Wastewater	0	0	-	-	0
		40	41.11	102.8	1.43	41.35
		60	61.15	102.0	0.61	61.50
		80	80.18	100.2	1.89	80.73
p-NP	Industrial Wastewater	0	2.32		0.21	2.57
		40	43.98	103.9	0.56	43.16
		60	63.96	102.6	0.80	63.67
		80	83.71	101.7	1.31	83.93

Table S4 Recoveries of nitrophenol isomers for the lake water.

Detection	Samples	Spiked (μmol/L)	Found (μmol/L)	Recovery (%)	RSD (%) (n=6)
o-NP	Lake water	20	19.68	98.38	3.2
		75	74.60	99.47	3.7
		125	127.85	102.28	1.7
m-NP	Lake water	25	24.57	98.29	4.2
		75	74.71	99.61	2.5
		125	128.44	102.76	2.9
p-NP	Lake water	10	10.09	100.91	2.3
		20	19.97	99.83	4.3
		35	34.44	98.40	2.7

Table S5 Recoveries of nitrophenol isomers for the spiked tap water.

Detection	Samples	Spiked (μmol/L)	Found (μmol/L)	Recovery (%)	RSD (%) (n=6)
o-NP	Tap water	20	20.42	102.10	3.2
		75	75.53	100.7	3.0
		125	124.6	99.72	3.1
m-NP	Tap water	25	25.47	101.9	3.6
		75	74.22	98.96	2.1

		125	124.6	99.66	3.3
p-NP	Tap water	10	9.57	95.67	2.2
		20	19.21	96.05	1.1
		35	35.45	101.3	2.1

Table S6 Recovery of nitrophenol isomers from industrial wastewater (in the lab from the school of chemistry).

Detection	Samples	Spiked (μmol/L)	Found (μmol/L)	Recovery (%)	RSD (%) (n=6)
o-NP (Chem lab)	Industrial Wastewater	0	0	-	-
		40	38.67	96.68	3.18
		60	61.40	102.3	2.63
		80	83.18	104.0	0.94
m-NP (Chem lab)	Industrial Wastewater	0	-	-	-
		40	38.30	95.75	2.64
		60	57.84	96.40	1.01
		80	81.50	101.9	3.84
p-NP (Chem lab)	Industrial Wastewater	0	1.97	-	1.29
		40	40.64	101.6	1.14
		60	62.05	103.4	0.94
		80	81.51	101.9	2.40

Quantum yield:
The relative quantum yield was determined according to the equation:

$$\phi_{un} = \phi_{std} \cdot \frac{F_{un}}{F_{std}} \cdot \frac{A_{std}}{A_{un}} \cdot \left(\frac{\eta_{un}}{\eta_{std}}\right)^2$$

Where std represents the reference of quine sulfate, and un represents the sample. F is the integral photon fluxes emitted from the sample (or the quantum yield standard) from the spectrally corrected spectra. A is the absorbance at the excitation wavelength, and η is the refractive index of solvent. Quinine sulfate solution (dissolved at 0.10 M H_2SO_4) was used as the standard (ϕ_{std} = 0.54, η = 1.33). To minimize re-absorption effects, absorbances in the 10

mm fluorescence cuvette were kept less than 0.1 at the excitation wavelength. The quantum yield of SQDs is calculated as 0.030 from the above equation.

References

1. Li, Y.; Ma, Y.; Lichtfouse, E.; Song, J.; Gong, R.; Zhang, J.; Wang, S.; Xiao, L., In situ electrochemical synthesis of graphene-poly(arginine) composite for p-nitrophenol monitoring. *Journal of Hazardous Materials* **2022,** *421*, 126718.
2. Liu, Q.; Zhao, F.; Shi, B.; Lu, C., Mussel-inspired polydopamine-encapsulated carbon dots with dual emission for detection of 4-nitrophenol and Fe(3). *Luminescence* **2021,** *36* (2), 431-442.
3. Das, D.; Dutta, R. K., N-Doped Carbon Dots Synthesized from Ethylene Glycol and β-Alanine for Detection of Cr(VI) and 4-Nitrophenol via Photoluminescence Quenching. *ACS Applied Nano Materials* **2021,** *4* (4), 3444-3454.
4. Wang, K.; Tan, L.; Zhang, Y.; Zhang, D.; Wang, N.; Wang, J., A molecular imprinted fluorescence sensor based on carbon quantum dots for selective detection of 4-nitrophenol in aqueous environments. *Marine Pollution Bulletin* **2023,** *187*, 114587.
5. Lin, Y.-C.; Lin, P.-Y.; Beck, D. E.; Hsu, Y.-C.; Cheng, S.-H.; Hsieh, S., Fluorescence quenching detection of p-nitrophenol in river water using functional perovskite quantum dots. *Environmental Technology & Innovation* **2023,** *32*, 103297.
6. Zhang, M.-Y.; Yi, F.-Y.; Liu, L.-J.; Yan, G.-P.; Liu, H.; Guo, J.-F., An europium(iii) metal–organic framework as a multi-responsive luminescent sensor for highly sensitive and selective detection of 4-nitrophenol and I− and Fe3+ ions in water. *Dalton Transactions* **2021,** *50* (43), 15593-15601.
7. Qiu, N.; Liu, Y.; Xiang, M.; Lu, X.; Yang, Q.; Guo, R., A facile and stable colorimetric sensor based on three-dimensional graphene/mesoporous Fe3O4 nanohybrid for highly sensitive and selective detection of p-nitrophenol. *Sensors and Actuators B: Chemical* **2018,** *266*, 86-94.
8. You, Y.; Li, S.-N.; Zou, J.; Xin, Y.-N.; Peng, S.; Liu, B.; Jiang, X.-Y.; Yu, J.-G., Ultrasonic-assisted self-assembly of a neodymium vanadate and hydroxylated multi-walled carbon nanotubes composite for electrochemical detection of p-nitrophenol. *Process Safety and Environmental Protection* **2023,** *175*, 834-844.
9. Lawaniya, S. D.; Pandey, G.; Yu, Y.; Awasthi, K., Efficient detection of p-nitrophenol via a polypyrrole flower-decorated nickel foam-based electrochemical sensor. *Nanoscale* **2024**.